

## RESEARCH ARTICLE

10.1002/2015JD024553

## Key Points:

- Observations show that CO<sub>2</sub> in the lower thermosphere has increased rapidly since the early 2000s
- The observed behavior cannot be simulated by a comprehensive climate-chemistry model
- Model and observations could be reconciled if vertical eddy mixing has increased by 30% per decade

## Correspondence to:

R. R. Garcia,  
rgarcia@ucar.edu

## Citation:

Garcia, R. R., M. López-Puertas, B. Funke, D. E. Kinnison, D. R. Marsh, and L. Qian (2016), On the secular trend of CO<sub>x</sub> and CO<sub>2</sub> in the lower thermosphere, *J. Geophys. Res. Atmos.*, 121, 3634–3644, doi:10.1002/2015JD024553.

Received 23 NOV 2015

Accepted 23 MAR 2016

Accepted article online 30 MAR 2016

Published online 8 APR 2016

On the secular trend of CO<sub>x</sub> and CO<sub>2</sub> in the lower thermosphere

Rolando R. Garcia<sup>1</sup>, Manuel López-Puertas<sup>2</sup>, Bernd Funke<sup>2</sup>, Douglas E. Kinnison<sup>1</sup>, Daniel R. Marsh<sup>1</sup>, and Liying Qian<sup>1</sup>

<sup>1</sup>National Center for Atmospheric Research, Boulder, Colorado, USA, <sup>2</sup>Instituto de Astrofísica de Andalucía, CSIC, Granada, Spain

**Abstract** An analysis of recent observations (2004–2013) made by the Atmospheric Chemistry Experiment Fourier Transform Spectrometer (ACE-FTS) instrument indicate that total carbon (CO<sub>x</sub> = CO + CO<sub>2</sub>) has been increasing rapidly in the lower thermosphere, above 10<sup>-3</sup> hPa (90 km). The estimated trend (~9% per decade) is about a factor of 2 larger than the rate of increase that can be ascribed to anthropogenic emissions of CO<sub>2</sub> (~5% per decade). Here we investigate whether the observed trends of CO<sub>2</sub> and CO<sub>x</sub> can be reproduced using the Whole Atmosphere Community Climate Model (WACCM), a comprehensive global model with interactive chemistry, wherein vertical eddy diffusion is estimated from a parameterization of gravity wave breaking that can respond to changes in the model climate. We find that the modeled trends of CO<sub>2</sub> and CO<sub>x</sub> do not differ significantly at any altitude from the value expected from anthropogenic increases of CO<sub>2</sub> and that WACCM does not produce significant changes in eddy diffusivity. We show that the discrepancy between model and observations cannot be attributed to uncertainties associated with geophysical noise and instrumental effects, to difficulties separating a linear trend from the 11 year solar signal, or to sparse sampling by ACE-FTS. Estimates of the impact of vertical diffusion on CO<sub>2</sub> in the model indicate that a large increase in K<sub>zz</sub> (~30% per decade) would be necessary to reconcile WACCM results with observations. It might be possible to ascertain whether such a large change in vertical mixing has in fact taken place by examining the trend of water vapor in the upper mesosphere.

## 1. Introduction

*Emmert et al.* [2012] calculated the global linear trend of CO<sub>x</sub> (the sum of CO and CO<sub>2</sub>) from observations made by the Atmospheric Chemistry Experiment Fourier Transform Spectrometer (ACE-FTS) between April 2004 and September 2011 and documented a very fast rate of increase at altitudes above about 10<sup>-3</sup> hPa (~90 km). Near 100 km, the linear trend of CO<sub>x</sub> was approximately 9% per decade, which is much faster than the anthropogenic rate of increase of CO<sub>2</sub> in the lower atmosphere for the period in question (~5% per decade). *Emmert et al.* [2012] analyzed the trend in CO<sub>x</sub> in order to minimize the effects of the solar cycle on CO<sub>2</sub>, since the photolysis of this gas by UV radiation (which produces CO) becomes important above 90 km and varies strongly with solar activity. Insofar as CO<sub>2</sub> represents the bulk of CO<sub>x</sub> below about 100 km, *Emmert et al.* [2012] ascribed the trend in CO<sub>x</sub> to increases in CO<sub>2</sub>. They also showed, using a one-dimensional model with interactive chemistry [Roble, 1995], that the observed trend in CO<sub>x</sub> could be due to a corresponding trend in vertical eddy diffusion of 15% per decade, since such a trend would increase the rate of transport of CO<sub>2</sub> into the lower thermosphere. Indeed, *Garcia et al.* [2014] have shown that in the range of altitude 90–105 km (about 10<sup>-3</sup> to 10<sup>-4</sup> hPa), the mixing ratio of CO<sub>2</sub> is controlled principally by the competition between eddy diffusion and molecular diffusive separation.

*Emmert et al.*'s [2012] conclusions regarding a fast rate of increase of CO<sub>2</sub> in the lower thermosphere are supported by the recent study of *Yue et al.* [2015], who used SABER (Sounding of the Atmosphere by Broadband Emission Radiometry) observations from 2002 to 2014, and estimated a rate of increase of CO<sub>2</sub> exceeding 10% per decade above 100 km. While SABER observations do not include CO, *Yue et al.* [2015] performed a multiple linear regression that included the solar 10.7 cm radio flux as a predictor to account for the influence of solar activity on CO<sub>2</sub>.

Here we investigate whether the large trends of CO<sub>2</sub> and CO<sub>x</sub> in the upper atmosphere derived from observations can be reproduced in simulations made with the Whole Atmosphere Community Climate Model (WACCM), a three-dimensional, global climate model with interactive chemistry. The model is discussed briefly in section 2, with emphasis on the question of transport in the mesosphere and lower thermosphere

(MLT), which is dominated by the divergence of vertical eddy fluxes due to breaking gravity waves. While these small-scale waves cannot be simulated explicitly at the relatively coarse spatial and temporal resolutions used in a climate model, they are parameterized in such a way that they can respond to changes in the model's climate.

In section 3, we compare updated ACE-FTS observations that span the period 2004 through 2013 with WACCM simulations of the same period to show that the simulated CO and CO<sub>2</sub> agree well with the observations in the lower thermosphere. In section 4, we derive trends in CO<sub>x</sub> and CO<sub>2</sub> from the ACE-FTS data and compare them with trends derived from WACCM output, and with the earlier estimates of *Emmert et al.* [2012]. The trends derived from the data are consistent with the findings of *Emmert et al.* [2012] and are much larger than the model trends above 90 km. In fact, WACCM-derived trends in the lower thermosphere are not significantly different from the trends below the mesopause, which are ascribable to anthropogenic emissions of CO<sub>2</sub>. We go on to examine several possible sources of uncertainty that might account for the discrepancy between observed and modeled trends and conclude that none can explain the differences between the model and the observations. Finally, we estimate the impact of increases in vertical eddy diffusion on the trends computed with WACCM and find that a rather large  $K_{zz}$  trend, of over 30% per decade, would be needed to reconcile the model with the observations. In section 5, we summarize our findings and suggest additional observations that might be useful for ascertaining whether such increases in vertical eddy diffusion might have taken place in the Earth's upper atmosphere.

## 2. Numerical Model

The Whole Atmosphere Community Climate Model (WACCM) is a global climate model with interactive chemistry that spans the range of altitude 0–140 km. In this study, we use the “specified dynamics” version (SD-WACCM), described by *Garcia et al.* [2014]. In SD-WACCM, winds and temperature are constrained by NASA's Modern-Era Retrospective Analysis data [*Rienecker et al.*, 2011] everywhere below approximately 1 hPa, using the procedure discussed by *Kunz et al.* [2011]. The use of SD-WACCM for the present investigation is motivated by the desire to study the particular period, 2004 through 2013, covered by the ACE-FTS observations described in the next section. While SD-WACCM is free running above 1 hPa, *Liu et al.* [2009] have shown that the dynamics of the mesosphere and lower thermosphere are strongly influenced by the behavior of the lower atmosphere. In the remainder of this paper, we refer to the model simply as WACCM, with the understanding that all simulations have been carried out with the specified dynamics version.

The reader is referred to the study of *Garcia et al.* [2014] for additional details of the specified dynamics configuration. Here we emphasize only the parameterization of small-scale gravity waves, since vertical mixing due to gravity wave breaking is the principal upward transport mechanism in the lower thermosphere, below 10<sup>-4</sup> hPa, particularly in the global-mean sense. The gravity wave parameterization attempts to take into account the excitation of mesoscale waves by various physical mechanisms, such as flow over orography, deep convection, and frontal zones. Nonorographic gravity wave source spectra are dependent on convective heat release in the tropics and frontal zones diagnosed in extratropical latitudes, as described in detail by *Richter et al.* [2010]. Because parameterized gravity wave sources are related to physical processes simulated in the underlying global model, their behavior can potentially change as the model climate changes. For example, the source spectra will change if the characteristics of convection or the frequency or intensity of fronts diagnosed in the model changes; and the propagation of the waves to the MLT will be influenced by the behavior of the zonal mean zonal wind systems in the stratosphere.

We note that the effective value of  $K_{zz}$  calculated with WACCM depends also on the value assumed for the Prandtl number,  $Pr$ , which describes the ratio of the eddy momentum flux to the eddy flux of potential temperature or chemical species [see *Garcia et al.*, 2007]. The value used in the study of *Garcia et al.* [2014] was  $Pr = 4$ . As discussed in that study, comparison of simulated and observed CO and CO<sub>2</sub> suggests that a smaller value,  $Pr = 2$ , might be more appropriate; therefore, we use simulations made with  $Pr = 2$  to compute model trends in this study. Nevertheless, in section 4 we use results from our earlier simulation with  $Pr = 4$  to estimate the potential impact of changes in  $K_{zz}$  on the trends of CO<sub>x</sub> and CO<sub>2</sub>. (It should be emphasized, however, that the trends of CO<sub>2</sub> and CO<sub>x</sub> in WACCM are insensitive to  $Pr$  as long as the value of  $Pr$  is constant throughout the simulation).

### 3. Comparison of Observed and Modeled CO and CO<sub>2</sub>

The Atmospheric Chemistry Experiment Fourier Transform Spectrometer (ACE-FTS) on SCISAT-1 has been making solar occultation measurements of CO and CO<sub>2</sub> since 2004 [Boone *et al.*, 2005; Clerbaux *et al.*, 2008; Beagley *et al.*, 2010]. CO<sub>2</sub> volume mixing ratio (vmr) is retrieved from 50 to 120 km; the vertical resolution averages 3–4 km, varying from 2 to 6 km depending on the time of the year. Random errors are 2.5–5%, depending on latitude, and systematic errors range from 2% at the low altitudes (50–70 km) to about 5% at 90 km, 9% at 100 km, and 16% at 118.5 km [Beagley *et al.*, 2010]. CO vmr is retrieved in the range from 8 km to about 100 km [Clerbaux *et al.*, 2008]. The vertical resolution above about 1 hPa is about 4 km, degrading to 6 km in the upper mesosphere. The random errors of the CO measurements are < 10% in the mesosphere and lower thermosphere; systematic errors are < 25% from 30 to 100 km. The ACE-FTS observations, as well as the data screening procedures employed, are discussed in more detail by Garcia *et al.* [2014]. The data used here are version 3.5 [Boone *et al.*, 2013] and were obtained from the ACE Science Team at the University of Waterloo, Canada. We note that ACE observations are processed in geometric coordinates. However, the final data products are provided in both geometric and pressure coordinates, and we use data in pressure coordinates in all comparisons with WACCM.

CO has also been observed by the Michelson Interferometer for Passive Atmospheric Sounding (MIPAS) using the “middle atmosphere” and “upper atmosphere” modes [Oelhaf, 2008], which cover the altitude ranges 20–102 km and 40–170 km, respectively. The vertical resolution of the MIPAS CO profiles is 4–7 km below 60 km at night and below 95 km during daytime, and 7–14 km above those altitudes. The single-measurement precision (noise error) is 40–80% below 60 km, and 30–60% above, while the systematic error is estimated to range between 8 and 15% [Funke *et al.*, 2009]. The MIPAS data are also discussed in detail by Garcia *et al.* [2014].

Figure 1 shows time series of WACCM CO and CO<sub>2</sub> together with observations at several levels in the lower thermosphere:  $6 \times 10^{-5}$  hPa (~108 km),  $2 \times 10^{-4}$  hPa (~100 km), and  $10^{-3}$  hPa (~90 km). For CO<sub>2</sub>, WACCM is within 10% of the ACE-FTS observations at all levels except  $6 \times 10^{-5}$  hPa, where the differences reach 15–20%. While the discrepancies are not large compared to the measurement errors for ACE-FTS, WACCM results for CO<sub>2</sub> are uniformly low in all cases. For CO, the WACCM simulation is generally closer to observations, especially given the large measurement errors. However, at  $10^{-3}$  hPa, WACCM CO is systematically higher than both ACE-FTS and MIPAS. In spite of these discrepancies, WACCM reproduces well the long-term variability of the data, which is dominated by the solar cycle, in particular at the higher altitudes.

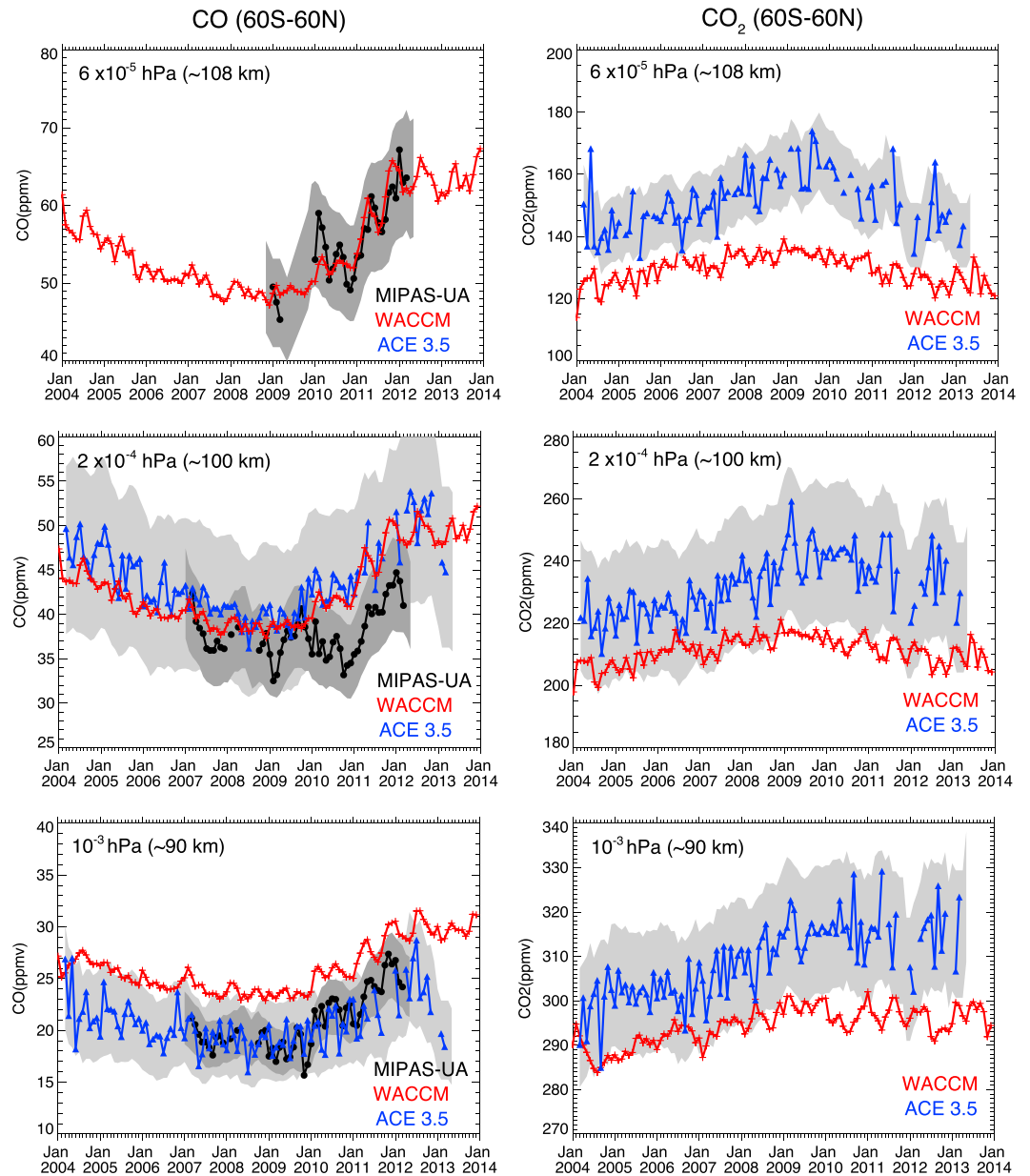
The effect of the solar cycle can be largely removed by considering total carbon, CO<sub>x</sub>, which in the lower thermosphere is essentially the sum of CO and CO<sub>2</sub>. Figure 2 shows a comparison of modeled and observed CO<sub>x</sub> at  $10^{-3}$  and  $2 \times 10^{-4}$  hPa, two levels where both CO and CO<sub>2</sub> are measured by ACE-FTS. Since CO<sub>x</sub> at these levels is dominated by CO<sub>2</sub>, the agreement is within 10%, as was the case for CO<sub>2</sub> in Figure 1, with WACCM being systematically low compared to ACE-FTS. In both model and observations, the evolution of CO<sub>x</sub> shows mainly an increasing trend, with no indication of any solar cycle influence. The rate of increase of CO<sub>x</sub> is clearly faster in ACE-FTS than in WACCM, and this difference will be quantified in the next section, where we calculate linear trends. An additional difference between model and observations, both for CO<sub>x</sub> and for CO and CO<sub>2</sub> individually, is that the observations exhibit considerably larger short-term variability than the model. The potential effect of this difference on the calculation of trends from WACCM output will be addressed below.

### 4. Calculation and Comparison of Linear Trends

Time series of CO<sub>x</sub> in WACCM are constructed from monthly mean, globally averaged output for CO and CO<sub>2</sub>. The model output was deseasonalized by subtracting the composite monthly seasonal cycle for the period 2004–2013 at each model level. ACE-FTS data were treated here in the same way as the WACCM output; that is, deseasonalized, global monthly averages were calculated from the data on each pressure level. This differs from the procedure employed by Emmert *et al.* [2012] but yields very similar trends, as shown below.

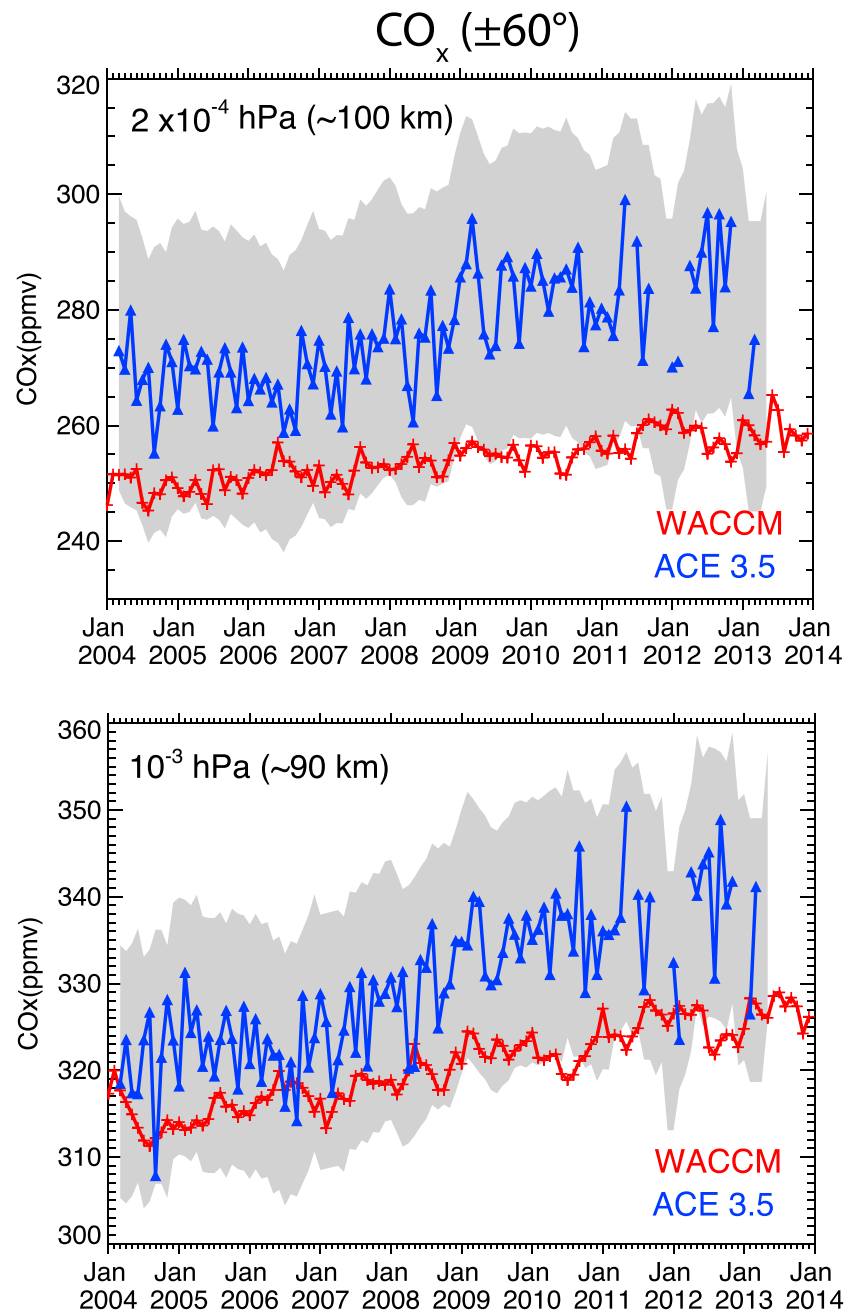
We characterize the long-term behavior of CO<sub>x</sub> in the 10 year period 2004 to 2013 in terms of the linear trend obtained from a multiple linear regression (MLR). The regression model used is

$$\psi = a + b \cdot t + c \cdot s(t) + d \cdot qbo_1(t) + e \cdot qbo_2(t), \quad (1)$$



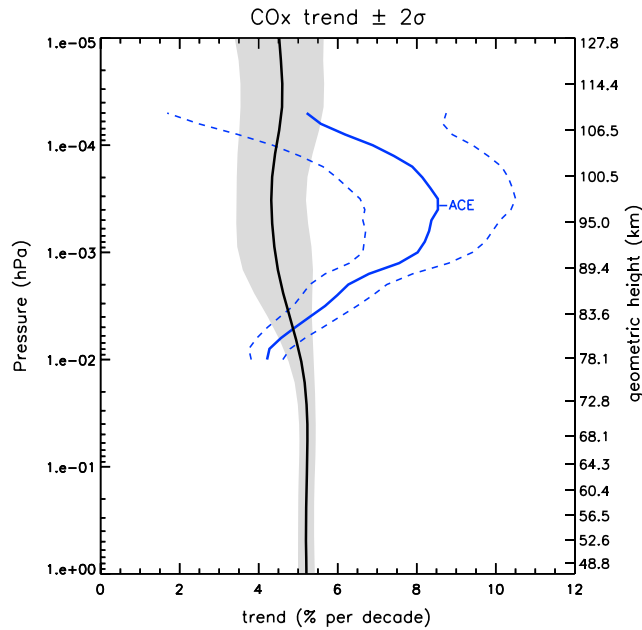
**Figure 1.** Evolution of observed and modeled (left) CO and (right) CO<sub>2</sub> averaged over 60°S–60°N for 2004–2013 at three pressure levels. Black and blue curves denote MIPAS and ACE data, respectively, with systematic measurement errors shaded; WACCM results are shown in red.

where  $t$  is time;  $s$  is a solar cycle predictor, here taken to be the 10.7 cm radio flux; and  $qbo_1$  and  $qbo_2$  are two linearly independent indices of the quasi-biennial oscillation (QBO), represented by the zonal mean zonal wind at 10 and 30 hPa, respectively. The autocorrelation of the residuals of the fit was taken into account when estimating the uncertainty of the trend [Tiao *et al.*, 1990]. No attempt was made to include in the MLR predictors for El Niño–Southern Oscillation or for volcanic eruptions. In practice, it turns out that even the QBO predictors explain a negligible fraction of the variance of CO<sub>x</sub> in the lower thermosphere. Likewise, the solar predictor turns out to be relatively unimportant at the altitudes (below about 105 km) where CO<sub>x</sub> data are available from ACE-FTS. Note that this is not true of CO<sub>2</sub> alone, which is photolyzed by UV radiation to produce CO. However, the combination of CO and CO<sub>2</sub> into a total carbon variable, CO<sub>x</sub>, has the desirable effect of minimizing the impact of the solar cycle on the MLR.



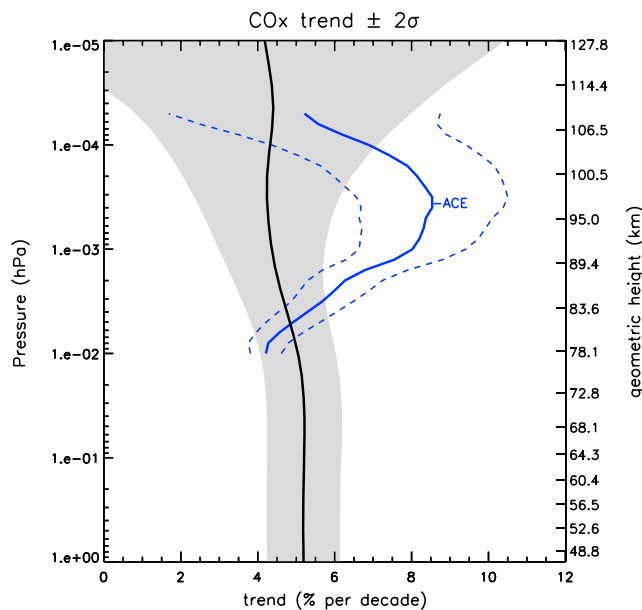
**Figure 2.** Evolution of observed and modeled  $\text{CO}_x$  averaged over  $60^\circ\text{S}$ – $60^\circ\text{N}$  for the period 2004–2013 at  $2 \times 10^{-4}$  hPa and  $10^{-3}$  hPa. Blue curves denote ACE data, with systematic errors shaded; WACCM results are shown in red.

Figure 3 compares the vertical profile of the linear trend coefficient,  $b$ , obtained when the MLR defined by equation (1) is applied to ACE-FTS observations and to WACCM output. Three things are immediately obvious from the figure: The trend calculated from ACE-FTS measurements reaches a maximum of 8.5% at 95–100 km, consistent with the results of Emmert *et al.* [2012], who analyzed a shorter period (2004–2011); the trend calculated from WACCM output in the lower thermosphere is statistically indistinguishable from the trend at lower altitudes; and the WACCM trend is significantly different from that derived from ACE-FTS observations in the lower thermosphere, between  $2 \times 10^{-3}$  hPa ( $\sim 85$  km) and  $2 \times 10^{-4}$  hPa ( $\sim 100$  km). As in Emmert *et al.* [2012], our estimate of the ACE-FTS trend below 80 km ( $\sim 10^{-2}$  hPa) is influenced by a priori assumptions about  $\text{CO}_2$  inherent in the ACE-FTS retrieval, which yield too low a trend for the period under examination. However, as noted by Emmert *et al.* [2012], this does not affect the estimate of the trend above 90 km ( $\sim 10^{-3}$  hPa).



**Figure 3.** Vertical profile of the global trend (% per decade) of  $CO_x = CO + CO_2$  for the period 2004–2013 derived from ACE observations (blue) and WACCM results (black). Dashed lines and gray shading denote 2 sigma uncertainties of the ACE and WACCM trend estimates, respectively.

$CO$  and  $CO_2$  a series of normally distributed pseudorandom numbers, multiplied times the standard deviation of the original time series at each altitude; this has the effect of increasing the standard deviation of the resulting “noisy” time series by about a factor of  $\sqrt{2}$  compared to the original. As a result, the high-frequency variability of the treated WACCM output is similar to that seen in ACE-FTS data (not shown). The linear  $CO_x$  trend profile extracted from the WACCM output with added noise is shown in Figure 4.



**Figure 4.** Effect on the WACCM  $CO_x$  trend of adding random noise to the model output. The blue curve denotes the trend derived from ACE; dashed lines and gray shading denote 2 sigma uncertainties of the ACE and WACCM trend estimates, respectively. See text for details.

We consider next whether the statistical significance of the WACCM-ACE differences might be exaggerated because WACCM  $CO_x$  has substantially less short term variability than ACE-FTS data. Specifically, the WACCM time series shown in Figures 1 and 2 are constructed from true zonal means averaged globally over latitude, whereas ACE-FTS solar occultation observations are much more sparse, both in longitude and latitude, and in time, and they are subject to measurement errors not present in WACCM. A cursory examination of Figures 1 and 2 reveals that the high-frequency variability is about a factor of 2 larger in the ACE-FTS time series than in the WACCM time series. We therefore test the sensitivity of the WACCM trends to the addition of “random noise,” which we simulate simply by adding to the time series of WACCM

is much larger than for the original WACCM output (Figure 3), the trend in the thermosphere remains statistically undistinguishable from the trend at lower altitudes and statistically different from the ACE-FTS trend between about 85 and 100 km.

We have also tested whether uncertainties in our knowledge of 11 year solar variability at UV wavelengths might influence the  $CO_x$  trend derived from WACCM. As discussed by *Ermolli et al.* [2013], recent measurements of spectral solar irradiance (SSI) variability differ substantially from estimates based on empirical models. In particular, *Ball et al.* [2014] show that the 11 year variability observed by the SOLSTICE instrument onboard NASA’s *SORCE* satellite is much larger at wavelengths  $< 300$  nm than predicted by models such as *NRLSSI* [*Lean et al.*, 1997] and *SATIRE* [*Krivova et al.*, 2011]. For  $CO_x$ , we are interested in

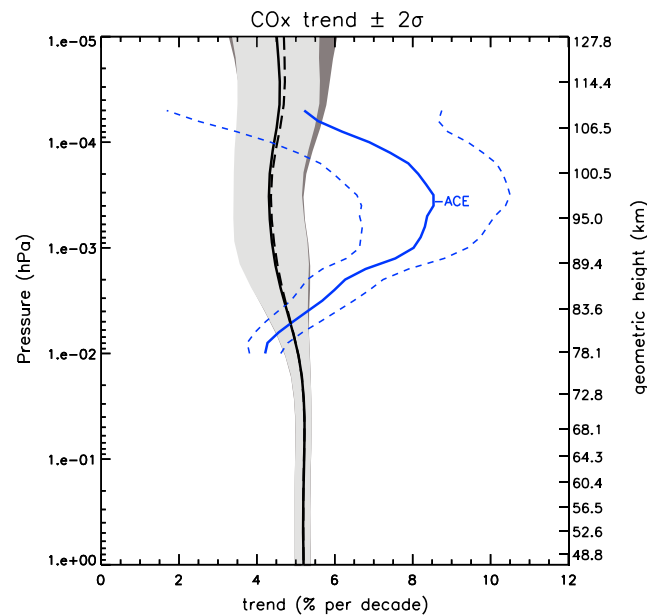


**Figure 5.** Effect on the WACCM  $\text{CO}_x$  trend of doubling the solar cycle irradiance variation at 120–200 nm. The solid curve and light shading denote the trend from the original simulation and its uncertainty; the dashed curved and dark shading refer to the simulation with increased irradiance variability. The blue curve and dashed lines denote the ACE trend and its uncertainty. See text for details.

[2014; cf. their Figure 9], the mixing ratio of  $\text{CO}_2$  below  $10^{-4}$  hPa ( $\sim 105$  km) is determined mainly by the competition between vertical eddy diffusion due to gravity wave breaking and molecular diffusive separation, with a smaller influence from UV photolysis.

Finally, we have considered whether the sparse sampling inherent in solar occultation observations might contribute to the differences in the trend profiles derived from ACE-FTS and WACCM. To investigate this possibility, we extracted WACCM vertical profiles of CO and  $\text{CO}_2$  at the geolocations (longitude, latitude, and time) nearest to ACE-FTS observations for the period 2004–2013. We then performed a trend analysis after processing the data as described by Emmert *et al.* [2012], with one exception: we regressed the WACCM output on both time (the linear trend) and on the solar  $F_{10.7}$  cm radio flux. As noted previously, regression on a solar predictor does not affect the results below  $10^{-4}$  hPa ( $\sim 105$  km), although it becomes increasingly important at higher altitudes, where  $\text{CO}_x$  is no longer conserved due to differences in molecular diffusion between CO and  $\text{CO}_2$ . The resulting trend profile is shown in Figure 6. It is clear that even when the model is sampled using the ACE geolocations, the WACCM trend is significantly smaller than the ACE-FTS trend at altitudes between about 85 and 100 km.

## 5. Summary and Discussion

The results presented above show that the global trend of  $\text{CO}_x$  in the lower thermosphere calculated with WACCM is not significantly different from the trend ascribable to anthropogenic increases in  $\text{CO}_2$  and that this trend (nowhere larger than 5.5%) is much smaller than the trend calculated from ACE-FTS observations (8–9% per decade in the lower thermosphere). We have also shown that even when we consider several plausible sources of uncertainty that might affect the WACCM  $\text{CO}_x$  trend, that trend remains smaller and statistically different from the ACE-FTS trend in the lower thermosphere.

Emmert *et al.* [2012] suggested that the  $\text{CO}_x$  trend derived from ACE-FTS observations could be explained if the rate of eddy diffusive transport of  $\text{CO}_2$  into the lower thermosphere was itself increasing. We have examined the evolution of the vertical diffusion coefficient,  $K_{zz}$ , estimated from the gravity wave

the range of wavelength 121–200 nm, which dominates  $\text{CO}_2$  photolysis below  $\sim 105$  km [cf. Garcia *et al.*, 2014; their Figure 1]. At these wavelengths, SSI changes over the 11 year solar cycle are about a factor of 2 larger in SOLSTICE observations than in either of the aforementioned models. SSI in WACCM is prescribed using the NRLSSI model, so we adjusted SSI variability in the range 120–200 nm to be twice as predicted by this model, with no changes elsewhere in the spectrum, and carried out a new simulation of the period 2004–2013. The resulting  $\text{CO}_x$  trend profile is compared with the original trend profile in Figure 5. It is evident that the larger SSI variability at 120–200 nm introduces little additional uncertainty in the WACCM  $\text{CO}_x$  trend, even at 100 km. This is not wholly surprising because the use of  $\text{CO}_x$  is intended to minimize the effect of solar variability on the estimate of the long-term trend. In addition, as shown by Garcia *et al.*

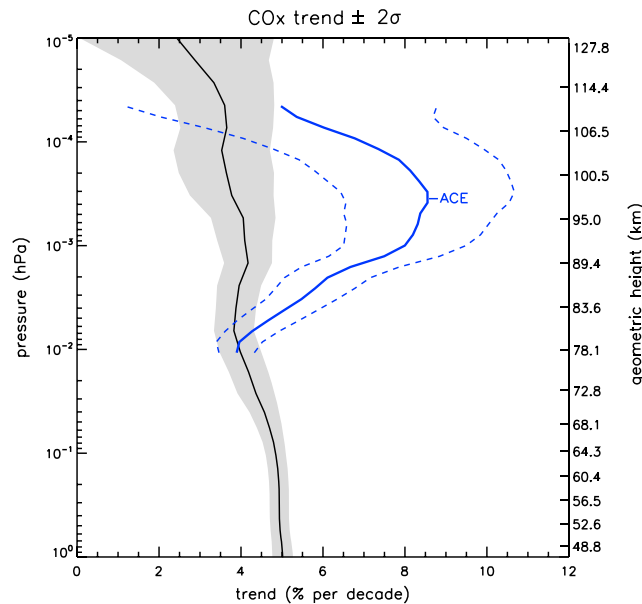


**Figure 6.** The WACCM CO<sub>x</sub> trend obtained when the model is sampled at the geolocations of the ACE-FTS observations compared with the trend obtained from ACE data; uncertainties are denoted by shading and dashed lines, respectively. See text for details.

magnitude of  $K_{zz}$  by approximately a factor of 2. As noted in section 2, the simulations examined thus far were made using  $Pr = 2$ , but we also have at hand earlier simulations, discussed by Garcia et al. [2014], that used  $Pr = 4$ . By comparing CO and CO<sub>2</sub> across the simulations, we can ascertain the impact of doubling  $K_{zz}$  on these species. Then, if we assume that changes in CO and CO<sub>2</sub> are linear in  $K_{zz}$ , we can estimate the impact of smaller changes in  $K_{zz}$  acting over one decade and thus estimate the decadal trend in eddy diffusion that is necessary to bring WACCM CO<sub>x</sub> trends into agreement with ACE-FTS trends.

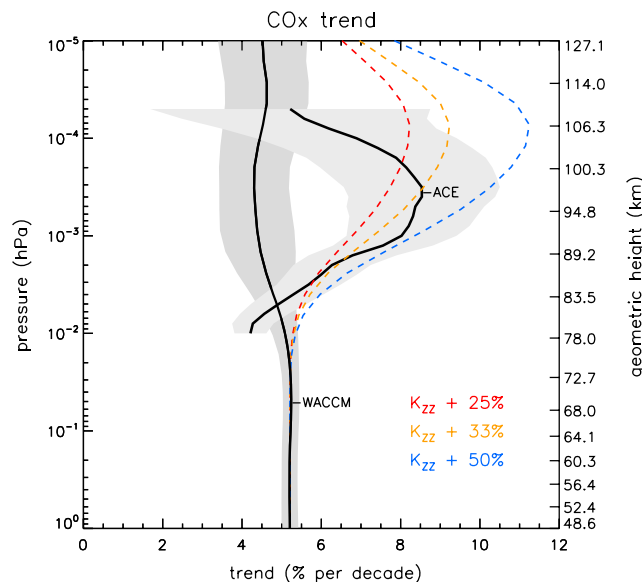


**Figure 7.** Effect of changing  $K_{zz}$  on the WACCM trend of CO<sub>x</sub>. ACE and WACCM trends for 2004–2013 are denoted by the black curves, with gray shading indicating 2 sigma uncertainties. The estimated impact on WACCM results of increasing  $K_{zz}$  by 25%, 33%, and 50% per decade is illustrated by the colored dashed curves. See text for details.

parameterization in WACCM and find no statistical significant trend anywhere in the model domain during the period under consideration, 2004–2013; this is consistent with the lack of any trend in CO<sub>2</sub> or CO<sub>x</sub> in the model beyond that due to anthropogenic emissions.

The value of  $K_{zz}$  in WACCM is predicted by the gravity wave parameterization interactively with the underlying, resolved dynamics, and cannot easily be adjusted ad hoc. However, we can estimate the impact of  $K_{zz}$  on chemical species by comparing otherwise identical simulations made with a different value of the Prandtl number,  $Pr$ , which describes the ratio of the eddy momentum flux to the eddy flux of chemical species [see Garcia et al., 2007]. In particular, halving  $Pr$  has the effect of increasing the effective

Figure 7 shows the estimated effect on the WACCM CO<sub>x</sub> trend of increasing  $K_{zz}$  at various rates. The figure reproduces the trend results shown earlier in Figure 3, superimposing upon those our estimates of the trends that would result if  $K_{zz}$  in WACCM increased at 25%, 33%, and 50% per decade. Above about  $10^{-2}$  hPa, where CO<sub>2</sub> is no longer well mixed, changes in  $K_{zz}$  begin to impact the CO<sub>x</sub> trend, and a trend of 33% per decade in  $K_{zz}$  gives the best match to the observed trend in CO<sub>x</sub> below about  $2 \times 10^{-4}$  hPa (95 km). Above that altitude there are substantial differences between the estimated WACCM trend and the ACE-FTS trend; better agreement might have been achieved by limiting the altitude range over which  $K_{zz}$  changes, but we have avoided any such arbitrary modifications, if for no

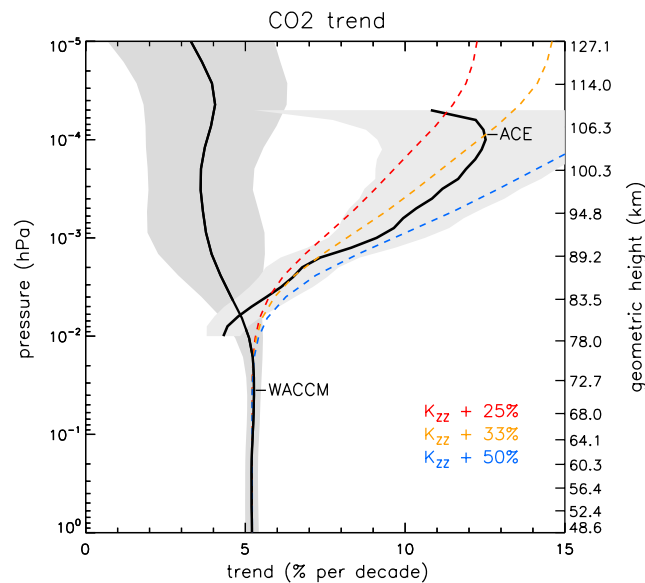


**Figure 8.** As in Figure 7, but for the trend of CO<sub>2</sub>.

with the trend obtained from ACE-FTS data. Incidentally, the ACE-FTS trend of CO is statistically indistinguishable from zero everywhere above 90 km (not shown). Thus, the discrepancy in modeled versus observed trends in CO<sub>x</sub> is dominated by the behavior of CO<sub>2</sub>, at least below 100–105 km, where most of the total carbon resides in CO<sub>2</sub>. The very large trend in CO<sub>2</sub> obtained from ACE-FTS data (which exceeds 12% near 105 km) is consistent with the recent study of *Yue et al.* [2015], who estimated the trend in CO<sub>2</sub> from observations made by the SABER instrument onboard NASA's TIMED satellite from 2002 to 2014. *Yue et al.* [2015] reported a trend of ~10% per decade above 105 km; as shown in their Figure 2, the trend profile derived from SABER differs from the ACE-FTS trend profile in that the trend peaks at a higher altitude but is consistent with ACE-FTS insofar as the trend in the lower thermosphere is much larger than the trend below 80 km.

Taken together, the SABER and ACE-FTS results make a strong case for a fast increase in CO<sub>2</sub> in the lower thermosphere in recent years. WACCM simulations, on the other hand, produce trends that are everywhere indistinguishable from the trend at lower altitudes, which can be ascribed to anthropogenic emissions of CO<sub>2</sub>. Estimates of the impact of  $K_{zz}$  on modeled trends suggest that an increase in eddy vertical mixing can bring the model results into agreement with observations. This is consistent with the conclusions of *Emmert et al.* [2012], who obtained a similar result using the one-dimensional, diffusive model of *Roble* [1995]. The required change in  $K_{zz}$  ranges from 15% per decade in the calculations of *Emmert et al.* [2012] to over 30% per decade in the estimates presented here. The parameterization of gravity wave breaking included in WACCM is designed to interact with the resolved dynamics of the underlying model, as discussed in section 2, but fails to produce a significant change in  $K_{zz}$  in the MLT over the period considered here (or indeed, over any period in the late twentieth and early 21st centuries; not shown). Furthermore, there is essentially no direct evidence for a recent global increase in turbulent mixing, although the work of *Hoffmann et al.* [2011] suggests a local increase in gravity wave activity over Juliusruh, Germany (55°N).

In view of the foregoing results, one might wonder whether it is possible to find additional, independent evidence for a rapid increase in eddy vertical mixing in the MLT since the early 2000s. Insofar as there are no global, long-term observations of gravity wave breaking in the MLT, evidence for a global increase in  $K_{zz}$  would have to come from global observations of minor species that are expected to respond sensitively to vertical mixing. We have examined the impact of  $K_{zz}$  in WACCM on several species, including atomic oxygen (which can be estimated from ozone and OH airglow observed by SABER, and is measured by the SCIAMACHY instrument on the Envisat satellite [*Zhu et al.*, 2015]), and water vapor (which has been measured by SABER but not yet released as a validated data product). As regards atomic oxygen, *Smith et al.* [2010] have

other reason that they would have required additional calculations that are not easily implemented in the model. A similar mismatch between the modeled and observed trend profiles occurred when *Emmert et al.* [2012] used a one-dimensional model to support their argument for an increase in the rate of vertical diffusion (cf. their Figure 2). Thus, neither the results presented in Figure 7 nor those of *Emmert et al.* [2012] produce a completely satisfactory agreement between modeled and observed trends of CO<sub>x</sub>, although they are able to match the observed trends over much of the lower thermosphere.

Similar results are obtained when trends in CO<sub>2</sub> alone are considered, as shown in Figure 8. Again, a decadal increase in  $K_{zz}$  of about a third would bring the WACCM trend of CO<sub>2</sub> into line

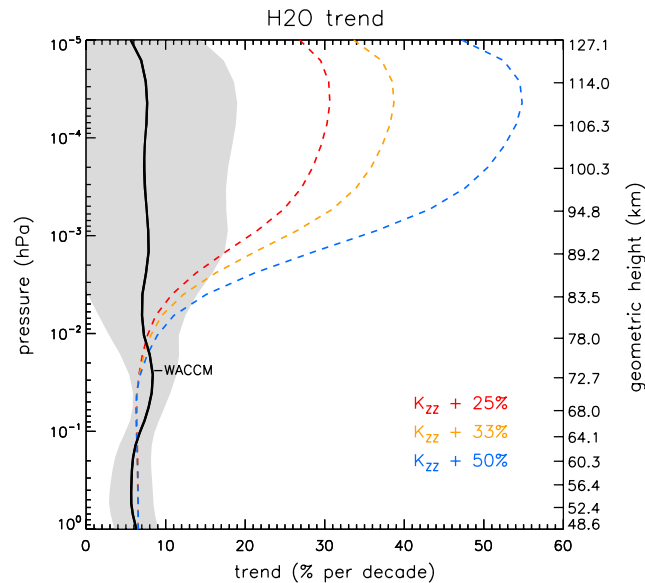


**Figure 9.** As in Figure 7, but for the trend of H<sub>2</sub>O.

is slow enough (days to weeks) that the vertical gradient is strongly influenced by eddy mixing. Figure 9 shows the estimated impact of trends in  $K_{zz}$  on the trend of water vapor. Between about 85 and 95 km ( $3 \times 10^{-3}$  to  $5 \times 10^{-4}$  hPa), where the H<sub>2</sub>O mixing ratio in WACCM varies from about 1 ppmv to 0.5 ppmv (not shown), a 33% per decade trend in  $K_{zz}$  would produce a trend in H<sub>2</sub>O varying from 15% per decade at 85 km to 30% per decade at 95 km. This is substantially larger than the trend below the mesopause ( $\sim 7\%$  per decade), which in WACCM arises mainly from specified anthropogenic emissions of methane and a slight warming of the cold point tropopause during the period of interest. Above 95 km, the trend in H<sub>2</sub>O produced by increasing  $K_{zz}$  is even larger than at lower altitudes, but the local mixing ratio is much less than 1 ppmv, likely making it impossible to retrieve its abundance accurately.

*Nedoluha et al.* [2009] studied the evolution of water vapor in the mesosphere, up to about 80 km, during solar cycle 23. They compared observations made by the Water Vapor Millimeter-wave Spectrometer (WVMS) with data from HALOE (Halogen Occultation Experiment) and other instruments that together covered the period 1992–2008. After accounting for the impact of changes in Lyman-alpha radiation over the solar cycle, *Nedoluha et al.* [2009] found that HALOE water vapor increased by about 8–9% between 60 and 80 km from 1992 to 1996; on the other hand, from 1996 to 2005 (the last year of HALOE observations), water vapor decreased slightly in both HALOE and WVMS. To put these findings in perspective, the WACCM water vapor trend over the decade 1992–2001 (which encompasses the period of increase documented by *Nedoluha et al.* [2009]) is  $\sim 8 \pm 7\%$  at 80 km and  $\sim 13 \pm 12\%$  at 90 km (not shown); this may be compared to the nearly altitude independent  $7 \pm 10\%$  per decade obtained for 2004–2013 (Figure 9). The trend in  $K_{zz}$  calculated by WACCM over the period 1992–2001 is also statistically indistinguishable from zero (not shown). Evidently, WACCM water vapor can exhibit substantial interdecadal variability, comparable to that seen in the observations analyzed by *Nedoluha et al.*, [2009] that is unrelated to eddy transport and could complicate the attribution of decadal trends. Nevertheless, the estimated impact of changes in  $K_{zz}$  illustrated in Figure 9 is large enough (15–30% per decade at 85–95 km) that it ought to be discernible even in the presence of variability arising from other sources.

In summary, the evidence from the observations considered in this study points to a fast rate of increase in CO<sub>2</sub> in the lower thermosphere that cannot be simulated with our state of the art climate-chemistry model. In order for WACCM to produce trends of CO<sub>x</sub> and CO<sub>2</sub> in the lower thermosphere consistent with ACE-FTS and SABER observations, vertical eddy diffusion would have to increase substantially (at an estimated rate of over 30% per decade). Examination of suitable data sets for other minor species (e.g., water vapor) in the lower thermosphere would be desirable to provide independent confirmation of such a rapid rate of increase in turbulent mixing.

shown that its vertical profile is affected by vertical diffusion. However, we find that even though O exhibits a very steep vertical gradient above 80 km, it is not very sensitive to changes in  $K_{zz}$  in WACCM. This happens because the vertical gradient of O is shallow at the altitudes where its photochemical lifetime is long, and steep mainly where it photochemical lifetime is short, which reduces the impact of transport on the local mixing ratio. Even a 50% change in  $K_{zz}$  produces changes in WACCM O whose magnitude is less than 10% (not shown).

Water vapor, on the other hand, may be a potentially useful indicator of changes in  $K_{zz}$ . Water vapor is photolyzed by Lyman-alpha radiation above about 80 km, but the rate of photolysis

## Acknowledgments

The Atmospheric Chemistry Experiment (ACE), also known as SCISAT, is a Canadian-led mission supported mainly by the Canadian Space Agency and the Natural Sciences and Engineering Research Council of Canada; we thank Kaley Walker for helping us access the ACE data and advising us on its use. We are also indebted to Anne K. Smith and William Randel for their comments and suggestions on the original version of this work and to Marty Mlynczak and two anonymous reviewers for their additional comments, all of which have resulted in an improved paper. The National Center for Atmospheric Research (NCAR) is sponsored by the U. S. National Science Foundation. R.R. Garcia and D.R. Marsh were supported in part by NASA grants X09AJ83G and NNX13AE33G, respectively. M. López-Puertas and B. Funke were supported by MINECO (Spain) under grant ESP2014-54362-P and EC FEDER funds. WACCM is a component of NCAR's Community Earth System Model (CESM), which is supported by the National Science Foundation (NSF) and the Office of Science of the U.S. Department of Energy. Computing resources were provided by NCAR's Climate Simulation Laboratory, sponsored by NSF and other agencies. This research was enabled by the computational and storage resources of NCAR's Computational and Information Systems Laboratory (CISL). The model output and data used in this paper are listed in the references or available from the authors.

## References

- Ball, W. T., N. A. Krivova, Y. C. Unruh, J. D. Haigh, and S. K. Solanki (2014), A new SATIRE-S spectral solar irradiance reconstruction for solar cycles 21–23 and its implications for stratospheric ozone, *J. Atmos. Sci.*, *71*, 4086–4101.
- Beagley, S. R., C. D. Boone, V. I. Fomichev, J. J. Jin, K. Semeniuk, J. C. McConnell, and P. F. Bernath (2010), First multi-year occultation observations of CO<sub>2</sub> in the MLT by ACE satellite: Observations and analysis using the extended CMAM, *Atmos. Chem. Phys.*, *9*, 1133–1153.
- Boone, C. D., R. Nassar, K. A. Walker, and Y. Rochon (2005), Retrievals for the atmospheric chemistry experiment Fourier-transform spectrometer, *Appl. Opt.*, *44*(33), 7218–7231.
- Boone, C. D., K. A. Walker, and P. F. Bernath (2013), Version 3 retrievals for the Atmospheric Chemistry Experiment Fourier Transform Spectrometer (ACE-FTS), in *The Atmospheric Chemistry Experiment ACE at 10: A Solar Occultation Anthology*, pp. 103–127, A. Deepak, Hampton, Va.
- Clerbaux, C., et al. (2008), CO measurements from the ACE-FTS satellite instrument: Data analysis and validation using ground-based, airborne and spaceborne observations, *Atmos. Chem. Phys.*, *8*, 2569–2594.
- Emmert, J. T., M. H. Stephens, P. F. Bernath, D. P. Drob, and C. D. Boone (2012), Observations of increasing carbon dioxide concentrations in the Earth's thermosphere, *Nat. Geosci.*, *5*, 868–871, doi:10.1038/ngeo1626.
- Ermolli, I., et al. (2013), Recent variability of the solar spectral irradiance and its impact on climate modeling, *Atmos. Chem. Phys.*, *13*, 3945–3977.
- Funke, B., M. López-Puertas, M. García-Comas, G. P. Stiller, T. von Clarmann, M. Höpfner, N. Glatthor, U. Grabowski, S. Kellmann, and A. Linden (2009), Carbon monoxide distributions from the upper troposphere to the mesosphere inferred from 4.7 μm non-local thermal equilibrium emissions measured by MIPAS on ENVISAT, *Atmos. Chem. Phys.*, *9*(7), 2387–2411.
- García, R. R., D. R. Marsh, D. E. Kinnison, B. A. Boville, and F. Sassi (2007), Simulation of secular trends in the middle atmosphere, 1950–2003, *J. Geophys. Res.*, *112*, D09301, doi:10.1029/2006JD007485.
- García, R. R., M. López-Puertas, B. Funke, D. R. Marsh, D. E. Kinnison, A. K. Smith, and F. González-Galindo (2014), On the distribution of CO<sub>2</sub> and CO in the mesosphere and lower thermosphere, *J. Geophys. Res. Atmos.*, *119*, 5700–5718, doi:10.1002/2013JD021208.
- Hoffmann, P., M. Rapp, W. Singer, and D. Keuer (2011), Trends of mesospheric gravity waves at northern middle latitudes during summer, *J. Geophys. Res.*, *116*, D00P08, doi:10.1029/2011JD015717.
- Krivova, N., S. K. Solanki, and Y. C. Unruh (2011), Towards a long-term record of solar total and spectral irradiance, *J. Atmos. Sol. Terr. Phys.*, *73*, 223–234, doi:10.1016/j.jastp.2009.11.013.
- Kunz, A., L. L. Pan, P. Konopka, D. E. Kinnison, and S. Tilmes (2011), Chemical and dynamical discontinuity at the extratropical tropopause based on START08 and WACCM analysis, *J. Geophys. Res.*, *116*, D24302, doi:10.1029/2011JD016686.
- Lean, J. L., G. J. Rottman, H. L. Kyle, T. N. Wood, J. R. Hickey, and L. C. Puga (1997), Detection and parameterization of variations in solar mid- and near-ultraviolet radiation (200–400 nm), *J. Geophys. Res.*, *102*, 29,329–29,956.
- Liu, H.-L., F. Sassi, and R. R. Garcia (2009), Error growth in a whole atmosphere climate model, *J. Atmos. Sci.*, *66*, 173–186.
- Nedoluha, G. E., R. M. Gomez, B. C. Hicks, J. E. Wrotny, C. Boone, and A. Lambert (2009), Water vapor measurements in the mesosphere from Mauna Loa over solar cycle 23, *J. Geophys. Res.*, *114*, D23303, doi:10.1029/2009JD012504.
- Oelhaf, H. (2008), MIPAS Mission Plan, *Tech. Note ENVI- SPPA-EOPG-TN-07-0073*, ESA.
- Richter, J. H., F. Sassi, and R. R. Garcia (2010), Toward a physically based gravity wave source parameterization in a general circulation model, *J. Atmos. Sci.*, *67*, 136–156.
- Rienecker, M. M., et al. (2011), MERRA: NASA's modern-era retrospective analysis for research and applications, *J. Clim.*, *24*, 3624–3648, doi:10.1175/JCLI-D-11-00015.1.
- Roble, R. G. (1995), Energetics of the mesosphere and thermosphere, in *The Upper Mesosphere and Lower Thermosphere: A Review of Experiment and Theory*, *Geophys. Monogr. Ser.*, vol. 87, edited by R. M. Johnson and T. L. Killeen, pp. 1–21, AGU, Washington, D. C., doi:10.1029/GM087p0001.
- Smith, A. K., D. R. Marsh, M. G. Mlynczak, and J. C. Mast (2010), Temporal variations of atomic oxygen in the upper mesosphere from SABER, *J. Geophys. Res.*, *115*, D18309, doi:10.1029/2009JD013434.
- Tiao, G. C., G. C. Reinsel, D. Xu, J. H. Pedrick, X. Zhu, A. J. Miller, J. J. DeLuise, C. L. Mateer, and D. J. Wuebbles (1990), Effects of autocorrelation and temporal sampling schemes on estimates of trend and spatial correlation, *J. Geophys. Res.*, *95*, 20,507–20,517.
- Yue, J., J. Russell III, Y. Jian, L. Rezac, R. Garcia, M. López-Puertas, and M. G. Mlynczak (2015), Increasing carbon dioxide concentration in the upper atmosphere observed by SABER, *Geophys. Res. Lett.*, *42*, 7194–7199, doi:10.1002/2015GL064696.
- Zhu, Y., M. Kaufmann, M. Ern, and M. Riese (2015), Nighttime atomic oxygen in the mesopause region retrieved from SCIAMACHY O(<sup>1</sup>S) green line measurements and its response to solar cycle variation, *J. Geophys. Res. Space Physics*, *120*, 9057–9073, doi:10.1002/2015JA021405.